



Lanostane-type triterpenoids from *Kadsura coccinea*



Zheng-Xi Hu^{a, b}, Xiao-Nian Li^{b, c}, Yi-Ming Shi^{b, c}, Wei-Guang Wang^{b, c}, Xue Du^{b, c}, Yan Li^{b, c}, Yong-Hui Zhang^{a, **}, Jian-Xin Pu^{b, c, *}, Han-Dong Sun^{b, c}

^a Hubei Key Laboratory of Natural Medicinal Chemistry and Resource Evaluation, School of Pharmacy, Tongji Medical College, Huazhong University of Science and Technology, Wuhan 430030, People's Republic of China

^b State Key Laboratory of Phytochemistry and Plant Resources in West China, Kunming Institute of Botany, Chinese Academy of Sciences, Kunming 650201, People's Republic of China

^c Yunnan Key Laboratory of Natural Medicinal Chemistry, Kunming Institute of Botany, Chinese Academy of Sciences, Kunming 650201, People's Republic of China

ARTICLE INFO

Article history:

Received 21 February 2017

Received in revised form

29 March 2017

Accepted 31 March 2017

Available online 2 April 2017

Keywords:

Kadsura coccinea

Lanostane-type triterpenoids

Cytotoxicity

ABSTRACT

Systematic phytochemical investigation on the stems of *Kadsura coccinea* resulted in the isolation of eleven new lanostane-type triterpenoids, named kadcoccinones G–Q (**1–11**), together with two known structural analogues, kadpolysperin M (**12**) and abiesatrane D (**13**). Their structures were characterized on the basis of comprehensive spectroscopic methods, and the absolute configuration of **1** was ascertained by single-crystal X-ray diffraction. Structurally, compounds **1/2**, **4/5**, and **6/7** were three pairs of C-12 epimers, respectively. Additionally, compounds **1–11** were evaluated for their in vitro cytotoxicity against the human tumor HL-60, SMMC-772, A-549, MCF-7, SW-480, and HeLa cell lines using the MTS viability assay.

© 2017 Elsevier Ltd. All rights reserved.

1. Introduction

Plants of the Schisandraceae family, consisting of two genera *Schisandra* and *Kadsura*, are well-known not only for the beneficial pharmacological activities, but also for their powerful abilities to produce architecturally attractive triterpenoids.^{1,2} Referring to their different carbon frameworks, Schisandraceae triterpenoids are classified into three categories: lanostane-type, cycloartane-type, and schinortriterpenoids (SNTs).^{1,2} Over the past decades, a series of studies have showed that SNTs were almost the chemotaxonomic markers for *Schisandra* species, and hitherto very few *Kadsura* species, such as *K. coccinea*³ and *K. ananosma*,⁴ involved the examples of SNTs, these results implied their intimate connections and huge differences. To further search for the relevance of these two genera, our research group has devoted itself to the discovery of structurally fascinating and bioactive secondary metabolites from the *Kadsura* species. Several highly oxygenated and rearranged lanostane-type or cycloartane-type triterpenoids with new

structural types were reported, such as kadlongilactones A and B,⁵ kadcoccinones A and B,⁶ kadcotrinones A–C,⁷ kadcoccinic acids A and B,⁸ and ananosins A–C,⁹ some of which showed cytotoxic or anti-HIV activities.

Kadsura coccinea (Lem.) A. C. Smith, distributed in southwest China, was commonly used in the Traditional Chinese Medicine (TCM) for the treatment of gastroenteric disorders and rheumatoid arthritis.³ Following a preliminary chemical investigation of the structurally novel and bioactive components of this species,^{10–12} eleven new lanostane-type triterpenoids (**1–11**) and two known structural analogues (**12** and **13**) were obtained from an EtOAc-soluble extract. In this report, the isolation, structure elucidation, and cytotoxicity for these compounds (Fig. 1) are described.

2. Results and discussion

Kadcoccinone G (**1**) was originally obtained as a white, amorphous powder. Its molecular formula was determined to be C₃₄H₅₂O₆ based on a [M + Na]⁺ ion at *m/z* 579.3658 in the HRESIMS analysis (calcd for C₃₄H₅₂O₆Na, 579.3656), indicative of nine degrees of unsaturation. The ¹H NMR spectroscopic data (Table 1) of **1** showed resonances characteristic for one doublet methyl (δ_{H} 0.98, *d*, *J* = 6.3 Hz), eight singlet methyls (δ_{H} 0.87, 0.90, 0.98, 1.03, 1.16, 2.01, 2.16, and 2.18), two olefinic protons (δ_{H} 5.66 and 6.05), and two

* Corresponding author. State Key Laboratory of Phytochemistry and Plant Resources in West China, Kunming Institute of Botany, Chinese Academy of Sciences, Kunming 650201, People's Republic of China.

** Corresponding author.

E-mail address: pujianxin@mail.kib.ac.cn (J.-X. Pu).

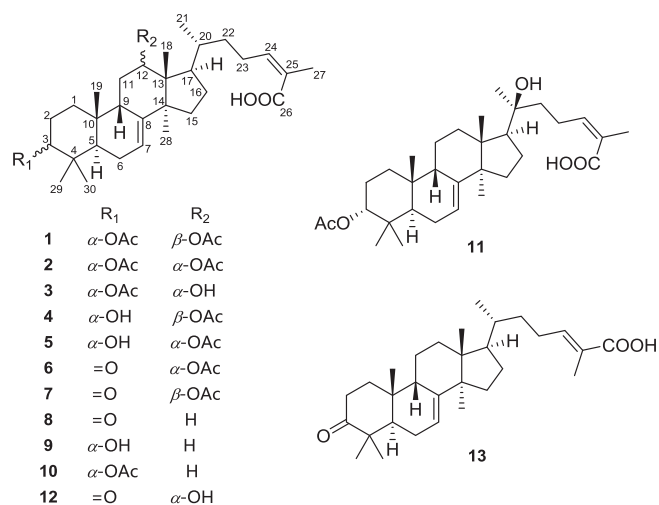


Fig. 1. Chemical structures of compounds 1–13.

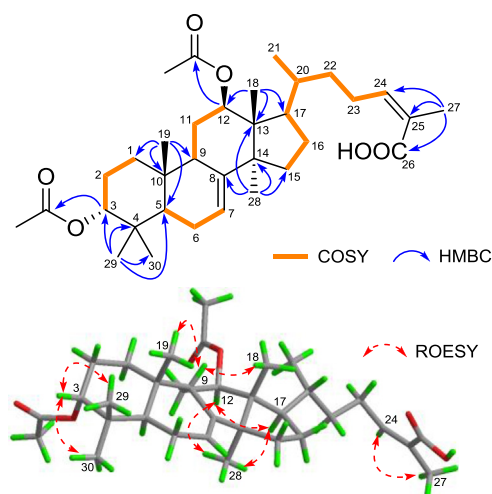


Fig. 2. Selected 2D NMR correlations of compound 1.

oxygenated methines (δ_{H} 4.82 and 5.28). Its ^{13}C NMR and DEPT data (Table 3) revealed 34 carbon resonances, corresponding to seven methyls, eight sp^3 methylenes, eight methines (two oxygenated and two olefinic), seven quaternary carbons [two olefinic and one carboxyl (δ_{C} 171.2)], and two acetyl groups (δ_{C} 170.8 C, 21.5 CH_3 ; 171.0 C, 22.2 CH_3). Apart from five degrees of unsaturation occupied by two double bonds and three carbonyls, the remaining ones required a tetracyclic structure for **1**.

These evidence indicated that compound **1** was an intact lanostane-type triterpenoid, whose ^1H and ^{13}C NMR spectroscopic data were very similar to those of kadcocconone F,¹⁰ differing only in that **1** possessed an acetyl group instead of a ketone group at C-12. This speculation was further supported by the 2D NMR spectra (Fig. 2), including ^1H – ^1H COSY cross-peaks of H-9/H₂-11/H-12 and

HMBC correlations from Me-18 to C-12 and from H-12 to the acetyl carbonyl (δ_{C} 171.0). Similar ROESY correlations clarified that the relative configuration of **1** was identical to that of kadcocconone F. Additionally, the apparent ROESY interactions (Fig. 2) of H-12, H-17 α , and Me-28 revealed that 12-OAc should be β -direction. Therefore, the relative configuration of **1** was determined.

By recrystallization with various organic solvents, a suitable crystal of **1** was obtained from CHCl_3 (with six drops of MeOH), which was then submitted to a single-crystal X-ray diffraction experiment (Fig. 3). A Flack parameter of 0.01(10) (CCDC 1470163) not only verified our speculation for its planar structure, but also undisputedly allowed an explicit assignment of its absolute structure as 3*R*,5*R*,9*S*,10*R*,12*R*,13*R*,14*S*,17*R*,20*R*, and a *Z*-geometry of the double bond between C-24 and C-25.

Table 1

^1H NMR spectroscopic data (δ in ppm, *J* in Hz) for compounds 1–5 in pyridine-*d*₅.

no.	1 ^{a,b}	2 ^{a,b}	3 ^{a,b}	4 ^{a,b}	5 ^{a,b}
1	1.03 m; 1.69 m	1.14 m; 1.74 m	1.22 m; 1.89 m	1.12 m; 2.30 m	1.17 m; 2.29 m
2	1.66 m; 1.80 m	1.68 m; 1.85 m	1.71 m; 1.89 m	1.78 m; 1.98 m	1.80 m; 2.01 m
3	4.82 br s	4.85 br s	4.85 br s	3.64 br s	3.65 br s
5	1.38 dd (10.0, 5.3)	1.43 br d (9.7)	1.50 dd (10.4, 5.0)	1.66 m	1.69 dd (11.0, 4.2)
6	1.89 m	1.91 m	1.94 m	1.99 m	2.01 m
7	5.66 m	5.72 m	5.75 m	5.71 m	5.76 m
9	2.59 br d (14.4)	2.33 br d (14.2)	2.41 m	2.62 m	2.33 m
11	1.87 m; 2.36 m	1.54 m; 2.82 m	1.91 m; 2.63 m	1.94 m; 2.37 m	1.46 m; 2.86 m
12	5.28 br d (7.2)	5.14 dd (9.8, 7.1)	4.20 t (7.9)	5.23 br d (7.2)	5.11 dd (9.0, 7.1)
15	1.58 m; 1.68 m	1.59 m	1.66 m	1.58 m; 1.70 m	1.60 m
16	1.41 m; 2.07 m	1.34 m; 2.11 m	1.41 m; 2.20 m	1.41 m; 2.06 m	1.32 m; 2.11 m
17	1.71 m	2.24 m	2.63 m	1.68 m	2.23 m
18	1.16 s	0.96 s	1.03 s	1.17 s	0.97 s
19	0.98 s	1.01 s	1.06 s	1.08 s	1.10 s
20	1.51 m	1.50 m	1.61 m	1.50 m	1.50 m
21	0.98 d (6.3)	0.94 m	1.36 d (6.6)	0.97 d (6.9)	0.93 d (6.7)
22	1.24 m; 1.69 m	1.29 m; 1.69 m	1.40 m; 1.80 m	1.25 m; 1.68 m	1.30 m; 1.69 m
23	2.78 m; 2.86 m	2.80 m; 2.87 m	2.89 m; 2.97 m	2.77 m; 2.86 m	2.78 m; 2.88 m
24	6.05 t (6.9)	6.07 t (6.2)	6.08 t (6.9)	6.05 t (7.0)	6.07 t (7.4)
27	2.16 s	2.15 s	2.14 s	2.15 s	2.15 s
28	1.03 s	1.17 s	1.47 s	1.01 s	1.14 s
29	0.87 s	0.89 s	0.90 s	0.96 s	0.98 s
30	0.90 s	0.93 s	0.93 s	1.24 s	1.26 s
–OAc	2.01 s	1.94 s	1.98 s	2.13 s	2.08 s
–OAc	2.18 s	2.07 s	–	–	–

^a Recorded at 600 MHz.

^b “m” means overlapped or multiplet with other signals.

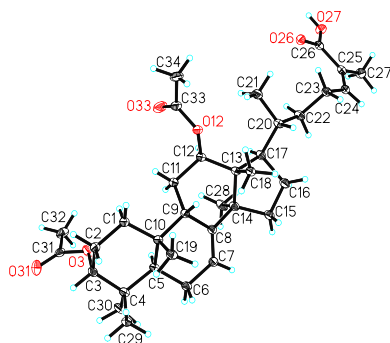


Fig. 3. X-ray crystallographic structure of compound **1**.

Kadcocconone H (**2**) had the same molecular formula as that of **1** ($C_{34}H_{52}O_6$), as assigned by the HRESIMS and ^{13}C NMR data. Side-by-side comparison of the 1D NMR spectroscopic data (Tables 1 and 3) of **2** with those of **1** indicated their structural similarities, belonging to a pair of C-12 epimers. Yet, the significant differences in carbon resonances between **2** and **1** at C-17 ($\Delta\delta_C = -9.0$ ppm) indicated the presence of a γ -steric compression effect between 12-OAc and H-17 α in **2**. Thus, the 12-OAc in **2** was deduced as α -oriented, which was supported by a key ROESY correlation (Fig. 4) of Me-18/H-12. Furthermore, the key ROESY cross-peaks (Fig. 4) of Me-29/H-3/Me-30, Me-29/H-2/Me-19 β , H-9 β /Me-18, Me-30/H-5 α , H-17 α /Me-28, and H-24/Me-27 suggested that the relative configuration of **2** was identical to that of **1**, with the only distinction that **1** had a 12 β -OAc group, while **2** had a 12 α -OAc group. Thus, the structure of **2** was identified as depicted.

Kadcocconone I (**3**) was obtained as a white, amorphous powder. Its molecular formula $C_{32}H_{50}O_5$ was assigned based on the HRESIMS analysis at m/z 513.3570 $[M-H]^-$ (calcd for $C_{32}H_{49}O_5$, 513.3585). The 1D (Tables 1 and 3) and 2D NMR data of **3** closely resembled those of **2**, with the significantly changed signals corresponding to an acetyl (δ_H 2.07; δ_C 170.3 and 21.8) substituent at C-12 (δ_C 78.3) and the HMBC correlation from H-12 (δ_H 5.14) to the acetyl group in **2** were absent in **3**, which allowed the assignment of a hydroxy group at C-12 (δ_C 75.6) in **3**. Furthermore, the completely consistent chemical shifts of C-17 (δ_C 45.6) in **2** and **3** indicated that a γ -steric compression effect should also exist between 12-OH and H-17 α in **3**. Thus, the 12-OH was determined to be α -oriented, which was further supported by the key ROESY correlation between H-12 and Me-18 (Fig. S24, Supporting Information). The ROESY experiment suggested that **3** possessed the same relative configuration as that of **2**. Accordingly, the structure of **3** was determined as depicted.

Kadcocconone J (**4**) was assigned as a molecular formula of $C_{32}H_{50}O_5$ on the basis of the HRESIMS data, showing a pseudo-molecular $[M + Na]^+$ ion peak at m/z 537.3550. Compound **4** released closely similar 1H and ^{13}C NMR spectroscopic data (Tables 1 and 3) in comparison to those of **1**, only being the presence of a hydroxy group at C-3 in **4** instead of the acetyl group in **1**.

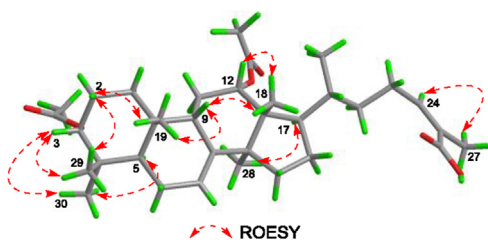


Fig. 4. Selected ROESY correlations of compound **2**.

This conclusion was further supported by the HMBC signals (Fig. 5) observed from Me-29 (δ_H 0.96) to C-3 (δ_C 75.6), C-4 (δ_C 38.4), and C-5 (δ_C 43.3), and from H-12 (δ_H 5.23) to the acetyl group (δ_C 170.8) in **4**. Along with the additional 1H - 1H COSY and HMBC correlations (Fig. 5), its gross structure was determined. Comparing **4** with kadcocconones D and E,¹⁰ the similar chemical shifts of C-3 ($\Delta\delta_C = 0.4$ ppm) indicated that the 3-OH in **4** should have identical α -orientations, which was supported by the key ROESY cross-peaks (Fig. 5) of Me-29/H-3/Me-30, Me-29/H-2/Me-19 β , and H-5 α /Me-30. Therefore, the structure of **4** was identified as depicted.

Kadcocconone K (**5**) possessed the same molecular formula as that of **4**, as inferred by analysis of the HRESIMS and ^{13}C NMR data. Examination of the 1H and ^{13}C spectroscopic data (Tables 1 and 3) of **5** with those of **4** suggested that they shared identical lanostane-type triterpenoid skeletons. The planar structure of **5** was equivalent to that of **4** by elaborative inspection of its 2D NMR (Fig. S40 and S41, Supporting Information) incorporating 1H - 1H COSY and HMBC correlations. Compared with **2** and **4**, the chemical shift at C-17 (δ_C 45.6) of **5** was identical to that of **2** ($\Delta\delta_C = 0$ ppm), whereas distinctly changeable to that of **4** ($\Delta\delta_C = -9.0$ ppm), indicating that a γ -steric compression effect between 12-OAc and H-17 α in **5** was assumed to exist. Hence, the 12-OAc in **5** should be α -oriented, which was further confirmed by a key ROESY correlation between H-12 and Me-18 (Fig. S42, Supporting Information). The relative configuration of **5** was identified to be identical to that of **2** by their closely related ROESY spectra. Accordingly, the structure of **5** was determined as depicted.

Kadcocconone L (**6**), obtained as a white, amorphous powder, displayed a quasi-molecular $[M + Na]^+$ ion at m/z 535.3394 (calcd for $C_{32}H_{48}O_5Na$, 535.3394) in the HRESIMS analysis, corresponding to a molecular formula of $C_{32}H_{48}O_5$, which was 2 mass units less than that of **5**. The 1H and ^{13}C NMR spectroscopic data (Tables 2 and 3) of **6** highly resembled those of **5**, with the diagnostic difference that a hydroxy group at C-3 in **5** was replaced by a ketone group (δ_C 218.1) in **6**, which was further supported by the observed signals that Me-29 (δ_H 1.13) and Me-30 (δ_H 1.11) correlated with C-3 (δ_C 218.1), C-4 (δ_C 47.4), and C-5 (δ_C 53.6) in the HMBC experiment (Fig. S49, Supporting Information). The similar ROESY spectra of **5** and **6** disclosed that they possessed consistent relative configurations. Thus, the structure of **6** was identified as depicted.

Kadcocconone M (**7**) was isolated as a white, amorphous powder with the same molecular formula $C_{32}H_{48}O_5$ as that of **6**. Analysis of the 1D (Tables 2 and 3) and 2D NMR data of **6** and **7** revealed that

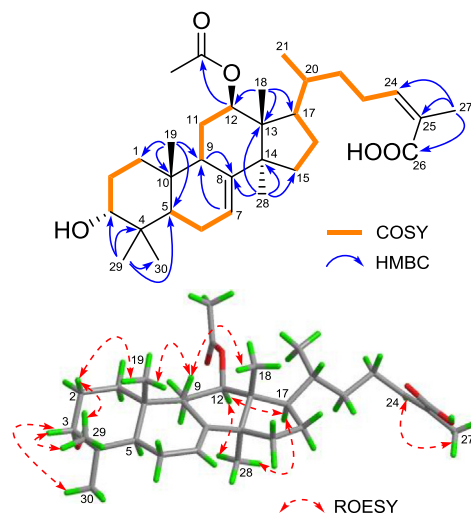


Fig. 5. Selected 2D NMR correlations of compound **4**.

Table 2
¹H NMR spectroscopic data (δ in ppm, *J* in Hz) for compounds **6–11** in pyridine-*d*₅.

no.	6 ^{a,b}	7 ^{a,b}	8 ^{a,b}	9 ^{a,b}	10 ^{a,b}	11 ^{a,b}
1	1.34 m; 1.54 m	1.37 m; 1.54 m	1.48 m; 1.65 m	1.25 m; 2.41 m	1.19 m; 1.85 m	1.21 m; 1.86 m
2	2.46 m; 2.58 m	2.50 m	2.52 m; 2.58 m	1.87 m; 2.08 m	1.75 m; 1.86 m	1.75 m; 1.87 m
3	–	–	–	3.68 br s	4.87 br s	4.87 br s
5	1.48 m	1.43 m	1.47 m	1.73 m	1.45 dd (9.4, 6.1)	1.47 dd (10.2, 5.1)
6	1.69 m; 1.90 m	1.77 m; 1.90 m	1.75 m; 1.89 m	2.02 m	1.91 m	1.92 m
7	5.73 m	5.69 m	5.68 m	5.71 m	5.66 m	5.71 m
9	2.19 m	2.46 m	2.18 m	2.38 m	2.36 m	2.47 br d (14.1)
11	1.53 m; 2.57 m	1.64 m; 2.33 m	1.54 m	1.58 m; 1.87 m	1.53 m; 1.81 m	1.61 m; 1.86 m
12	5.07 dd (9.1, 6.8)	5.31 br d (7.6)	1.54 m; 1.76 m	1.61 m; 1.70 m	1.64 m; 1.75 m	1.86 m; 1.94 m
15	1.47 m; 1.66 m	1.45 m; 1.75 m	1.44 m; 1.62 m	1.58 m	1.57 m	1.70 m; 1.79 m
16	1.40 m; 2.16 m	1.45 m; 2.09 m	1.33 m; 2.05 m	1.30 m; 2.02 m	1.30 m; 2.03 m	2.04 m; 2.41 m
17	2.36 m	1.79 m	1.57 m	1.49 m	1.51 m	2.05 m
18	0.79 s	1.02 s	0.79 s	0.97 s	0.96 s	1.52 s
19	0.89 s	0.90 s	0.95 s	1.14 s	1.04 s	1.04 s
20	1.50 m	1.52 m	1.48 m	1.50 m	1.51 m	–
21	0.97 d (6.6)	1.01 d (6.6)	1.00 d (6.4)	0.96 d (5.7)	0.98 d (5.5)	1.57 s
22	1.33 m; 1.72 m	1.28 m; 1.72 m	1.29 m; 1.70 m	1.26 m; 1.68 m	1.25 m; 1.68 m	1.89 m
23	2.82 m; 2.91 m	2.80 m; 2.88 m	2.81 m; 2.91 m	2.79 m; 2.89 m	2.79 m; 2.90 m	2.94 m; 3.08 m
24	6.08 t (7.4)	6.06 t (6.9)	6.06 t (6.4)	6.06 t (7.4)	6.06 t (7.0)	6.10 t (7.4)
27	2.18 s	2.17 s	2.17 s	2.15 s	2.16 s	2.14 s
28	1.21 s	1.03 s	1.03 s	1.03 s	1.04 s	1.17 s
29	1.13 s	1.10 s	1.14 s	0.99 s	0.91 s	0.91 s
30	1.11 s	1.11 s	1.12 s	1.27 s	0.94 s	0.95 s
–OAc	2.17 s	2.14 s	–	–	2.05 s	2.06 s

^a Recorded at 600 MHz.^b “m” means overlapped or multiplet with other signals.**Table 3**
¹³C NMR spectroscopic data (δ in ppm) for compounds **1–11** in pyridine-*d*₅.

no.	1 ^a	2 ^a	3 ^a	4 ^b	5 ^b	6 ^a	7 ^a	8 ^a	9 ^a	10 ^a	11 ^a
1	31.3 CH ₂	31.5 CH ₂	31.5 CH ₂	31.0 CH ₂	31.1 CH ₂	34.6 CH ₂	34.6 CH ₂	34.7 CH ₂	31.0 CH ₂	31.4 CH ₂	31.4 CH ₂
2	23.8 CH ₂	24.0 CH ₂	24.0 CH ₂	27.2 CH ₂	27.3 CH ₂	34.8 CH ₂	34.9 CH ₂	35.0 CH ₂	27.4 CH ₂	24.0 CH ₂	24.1 CH ₂
3	78.5 CH	78.4 CH	78.6 CH	75.6 CH	75.6 CH	218.1 C	217.6 C	218.1 C	75.7 CH	78.7 CH	78.7 CH
4	37.1 C	37.3 C	37.2 C	38.4 C	38.5 C	47.4 C	47.4 C	47.5 C	38.4 C	37.2 C	37.3 C
5	44.2 CH	44.9 CH	44.7 CH	43.3 CH	43.8 CH	53.6 CH	52.8 CH	53.1 CH	43.4 CH	44.3 CH	44.7 CH
6	23.7 CH ₂	23.6 CH ₂	23.7 CH ₂	24.0 CH ₂	24.0 CH ₂	23.5 CH ₂	23.7 CH ₂	23.6 CH ₂	24.0 CH ₂	23.7 CH ₂	23.8 CH ₂
7	122.7 CH	123.3 CH	122.5 CH	123.2 CH	123.7 CH	123.4 CH	122.9 CH	122.2 CH	122.6 CH	122.2 CH	122.3 CH
8	147.8 C	148.2 C	149.6 C	147.9 C	148.3 C	148.1 C	147.6 C	149.4 C	149.7 C	149.6 C	149.9 C
9	47.3 CH	47.1 CH	47.9 CH	47.6 CH	47.4 CH	44.4 CH	44.6 CH	46.1 CH	49.6 CH	49.3 CH	49.0 CH
10	36.0 C	36.4 C	36.4 C	36.3 C	36.7 C	36.4 C	36.2 C	36.4 C	36.6 C	36.4 C	36.4 C
11	35.3 CH ₂	32.3 CH ₂	36.3 CH ₂	35.4 CH ₂	32.5 CH ₂	30.5 CH ₂	32.8 CH ₂	21.4 CH ₂	23.8 CH ₂	23.7 CH ₂	23.8 CH ₂
12	76.3 CH	78.3 CH	75.6 CH	76.5 CH	78.5 CH	77.2 CH	76.2 CH	34.8 CH ₂	35.9 CH ₂	35.8 CH ₂	36.1 CH ₂
13	48.2 C	47.5 C	49.0 C	48.2 C	47.5 C	47.9 C	48.7 C	44.7 C	44.2 C	44.2 C	45.2 C
14	53.4 C	53.5 C	53.9 C	53.5 C	53.6 C	52.6 C	52.7 C	52.5 C	53.6 C	53.6 C	54.1 C
15	33.8 CH ₂	34.9 CH ₂	35.5 CH ₂	33.9 CH ₂	35.0 CH ₂	34.3 CH ₂	33.7 CH ₂	33.9 CH ₂	34.2 CH ₂	34.1 CH ₂	34.1 CH ₂
16	29.3 CH ₂	29.1 CH ₂	29.6 CH ₂	29.2 CH ₂	29.2 CH ₂	28.8 CH ₂	28.5 CH ₂	29.0 CH ₂	29.4 CH ₂	29.4 CH ₂	23.4 CH ₂
17	54.6 CH	45.6 CH	45.6 CH	54.6 CH	45.6 CH	44.9 CH	54.0 CH	53.6 CH	54.2 CH	54.3 CH	56.0 CH
18	16.1 CH ₃	22.6 CH ₃	23.0 CH ₃	16.1 CH ₃	22.6 CH ₃	20.5 CH ₃	15.2 CH ₃	23.0 CH ₃	24.4 CH ₃	24.4 CH ₃	25.8 CH ₃
19	24.6 CH ₃	24.7 CH ₃	24.9 CH ₃	25.0 CH ₃	25.2 CH ₃	23.3 CH ₃	23.4 CH ₃	23.6 CH ₃	25.3 CH ₃	24.9 CH ₃	25.0 CH ₃
20	35.9 CH	37.0 CH	37.8 CH	35.9 CH	37.0 CH	36.9 CH	35.8 CH	37.0 CH	37.0 CH	37.0 CH	74.6 C
21	18.9 CH ₃	18.4 CH ₃	18.5 CH ₃	18.9 CH ₃	18.4 CH ₃	18.4 CH ₃	19.0 CH ₃	19.0 CH ₃	19.0 CH ₃	19.0 CH ₃	27.1 CH ₃
22	36.5 CH ₂	36.5 CH ₂	36.9 CH ₂	36.6 CH ₂	36.6 CH ₂	36.6 CH ₂	36.5 CH ₂	36.7 CH ₂	36.6 CH ₂	36.6 CH ₂	45.2 CH ₂
23	27.7 CH ₂	27.7 CH ₂	28.2 CH ₂	27.7 CH ₂	27.7 CH ₂	27.6 CH ₂	27.7 CH ₂	27.6 CH ₂	27.7 CH ₂	27.7 CH ₂	26.1 CH ₂
24	143.0 CH	143.1 CH	143.4 CH	142.9 CH	143.1 CH	143.1 CH	143.0 CH	143.0 CH	143.2 CH	143.2 CH	143.4 CH
25	129.2 C	129.2 C	129.0 C	129.3 C	129.2 C	129.2 C	129.3 C	129.5 C	129.1 C	129.1 C	129.0 C
26	171.2 C	171.2 C	171.2 C	171.3 C	171.2 C	171.1 C	171.2 C	171.4 C	171.2 C	171.2 C	171.2 C
27	22.1 CH ₃	22.0 CH ₃	22.0 CH ₃	22.0 CH ₃	22.0 CH ₃	22.0 CH ₃	22.0 CH ₃	22.1 CH ₃	22.0 CH ₃	22.1 CH ₃	22.1 CH ₃
28	31.3 CH ₃	31.9 CH ₃	32.4 CH ₃	31.4 CH ₃	32.1 CH ₃	28.0 CH ₃	28.1 CH ₃	27.8 CH ₃	31.5 CH ₃	31.5 CH ₃	31.7 CH ₃
29	23.5 CH ₃	23.6 CH ₃	23.5 CH ₃	24.1 CH ₃	24.2 CH ₃	21.6 CH ₃	21.9 CH ₃	21.9 CH ₃	24.3 CH ₃	23.6 CH ₃	23.6 CH ₃
30	28.8 CH ₃	28.9 CH ₃	28.9 CH ₃	30.1 CH ₃	30.2 CH ₃	28.7 CH ₃	28.3 CH ₃	28.5 CH ₃	30.2 CH ₃	28.9 CH ₃	28.9 CH ₃
–OAc	170.8 C	170.8 C	170.8 C	170.8 C	170.2 C	170.4 C	171.0 C	–	–	170.9 C	170.8 C
–OAc	21.5 CH ₃	21.5 CH ₃	21.5 CH ₃	22.1 CH ₃	21.9 CH ₃	21.9 CH ₃	22.1 CH ₃	–	–	21.6 CH ₃	21.6 CH ₃
–OAc	171.0 C	170.3 C	–	–	–	–	–	–	–	–	–
–OAc	22.2 CH ₃	21.8 CH ₃	–	–	–	–	–	–	–	–	–

^a Recorded at 150 MHz.^b Recorded at 100 MHz.

they were a pair of C-12 epimers. The apparent variation ($\Delta\delta_C = 9.1$ ppm) for the chemical shifts of C-17 was observed between **6** (δ_C 44.9) and **7** (δ_C 54.0), indicating the absence of a γ -steric compression effect between 12-OAc and H-17 α in **7**. Accordingly, the 12-OAc in **7** should be assigned as β -oriented, which was confirmed by a key ROESY correlation of H-12 and Me-28 (Fig. S60, Supporting Information). Therefore, the structure of **7** was determined as depicted.

Kadcocconine N (**8**) was obtained as a white, amorphous powder and exhibited a molecular ion at m/z 453.3362 $[M - H]^-$ in the HRESIMS analysis, which correlated to a molecular formula of $C_{30}H_{46}O_3$. Analysis of the 1D (Tables 2 and 3) and 2D NMR spectroscopic data of **8** with those of **7**, revealed their structural similarities, except that an oxygenated methine (δ_C 76.2) and an acetyl group were absent and an sp^3 methylene (δ_C 34.8) at C-12 was present in **8**. This assumption was affirmed by the HMBC correlation of Me-18 (δ_H 0.79) with C-12 (Fig. S67, Supporting Information). The relative configuration of **8** was also determined to be identical to that of **7**, as inferred on the basis of the ROESY spectrum. Hence, the structure of **8** was identified as depicted.

The molecular formula of kadcocconine O (**9**) was deduced to be $C_{30}H_{48}O_3$ based on the HRESIMS data at m/z 455.3518 $[M - H]^-$ (calcd for $C_{30}H_{47}O_3$, 455.3531). 1D NMR spectroscopic data (Tables 2 and 3) revealed that **9** was a structural analogue of **4**, except for the disappearance of an acetyl group and an oxygenated methine (δ_C 76.5) and the presence of an sp^3 methylene (δ_C 35.9) at C-12 in **9**. The HMBC correlations (Fig. S76, Supporting Information) arising from Me-18 (δ_H 0.97) to C-12 (δ_C 35.9), C-13 (δ_C 44.2), C-14 (δ_C 53.6), and C-17 (δ_C 54.2) confirmed our conclusion. The ROESY spectrum of **9** highly resembled those of **4**, suggesting that they possessed identical relative configurations. Therefore, the structure of **9** was identified as depicted.

Kadcocconine P (**10**) gave a pseudo-molecular ion at m/z 497.3622 $[M - H]^-$ (calcd for $C_{32}H_{49}O_4$, 497.3636) in the negative HRESIMS analysis, corresponding to a molecular formula of $C_{32}H_{50}O_4$. The 1H and ^{13}C NMR spectroscopic data (Tables 2 and 3) of **10** were closely correlated with those of **1**, indicating that these two compounds possessed identical carbon skeletons and substitution patterns, except for the replacement of an acetyl group (δ_C 171.0 and 22.2) attached to an oxygenated methine (C-12) in **1** by an sp^3 methylene (δ_C 35.8) in **10**, which was supported by the observed $^1H-^1H$ COSY cross-peaks (Fig. S86, Supporting Information) of H-9/H₂-11/H₂-12, together with HMBC correlations (Fig. S85, Supporting Information) from Me-18 (δ_H 0.96) to C-12 (δ_C 35.8). Therefore, the structure of **10** was determined as depicted.

Kadcocconine Q (**11**) had a molecular formula of $C_{32}H_{50}O_5$ based on a pseudo-molecular ion at m/z 537.3551 $[M + Na]^+$ (calcd for $C_{32}H_{50}O_5Na$, 537.3550) in the positive HRESIMS analysis, which was 16 units greater than that of **10**. The 1H and ^{13}C NMR spectroscopic data (Tables 2 and 3) of **11** closely resembled those of **10**, implying that they shared the same A/B/C/D-ring systems and substitution patterns. Obviously, a doublet methyl (δ_H 0.98, $J = 5.5$ Hz; δ_C 19.0, C-21) and an sp^3 methine (δ_H 1.51; δ_C 37.0, C-20) signals disappeared in **10**, while a singlet methyl (δ_H 1.57; δ_C 27.1) and a downfield quaternary carbon (δ_C 74.6) signals were discovered in **11**, indicating that a hydroxyl group was attached to C-20, which was clearly supported by the observed HMBC signals (Fig. S94, Supporting Information) that Me-21 (δ_H 1.57), H₂-22 (δ_H 1.89), and H₂-23 (δ_H 2.94 and 3.08) correlated with C-20 (δ_C 74.6). By biosynthetic considerations^{1,2} and comparison of its ^{13}C NMR chemical shifts of C-20, C-21, and C-22 with those of dammarenediol I (20R), dammarenediol II (20S),¹³ and (2 β ,9 β ,10 α ,16 α ,20 β ,24Z)-2-(β -D-glucopyranosyloxy),¹⁴ the C-20 of **11** was determined to be S-configuration. Thus, the structure of **11** was defined as depicted.

The two known structural analogues were identified as kadpolysperin M (**12**)¹⁵ and abiesatrine D (**13**)¹⁶ by comparison of their spectroscopic data with those reported in the literature.

The structure–activity relationship of new compounds **1–11** were evaluated for their in vitro cytotoxicity against five human tumor cell lines: HL-60 (acute leukemia), SMMC-7721 (hepatic cancer), A-549 (lung cancer), MCF-7 (breast cancer), SW-480 (colon cancer), and HeLa (cervical cancer), using the MTS method as previously reported,¹⁷ with cis-platin as the positive control. As shown in Table 4, only compound **2** showed modest inhibitory effects with IC₅₀ values ranging from 13.43 to 37.94 μ M, indicating that two α -OAc substituent groups at both C-3 and C-12 could promote the cytotoxicity in this class of triterpenoids. And the pharmacological mechanism warrants further investigation.

3. Conclusion

From a chemotaxonomic view, lanostane-type triterpenoids occurred in the *Schisandra* and *Kadsura* species,^{1,2} implying the intimate connections of both genera. Our findings in this report would enrich our knowledge about the chemical diversity of triterpenoids in the Schisandraceae family.

4. Experimental section

4.1. General experimental procedures

Optical rotations were collected on a JASCO P-1020 digital polarimeter. UV spectra were measured using a Shimadzu UV-2401PC spectrophotometer. IR spectra were recorded on a Tenor 27 FT-IR spectrometer with KBr pellets. NMR spectra were obtained on Bruker AM-400 and DRX-600 spectrometers using TMS as internal standard. All chemical shifts (δ) were expressed in ppm with reference to the solvent signals for pyridine-*d*₅ (δ_H 8.74 and δ_C 150.35). HRESIMS data were performed on an API QSTAR Pulsar 1 spectrometer. Semi-preparative HPLC was carried out on an Agilent 1200 liquid chromatograph with Zorbax SB-C₁₈ (9.4 mm \times 250 mm) column. Column chromatography (CC) was performed with silica gel (200–300 mesh, Qingdao Marine Chemical, Inc., Qingdao, People's Republic of China) and Lichroprep RP-C₁₈ gel (40–63 μ m, Merck, Darmstadt, Germany). Thin-layer chromatography was performed on precoated TLC plates (200–250 μ m thickness, silica gel 60 F₂₅₄, Qingdao Marine Chemical, Inc.). Fractions were monitored by TLC and spots were visualized by heating silica gel plates sprayed with 10% H₂SO₄ in EtOH.

4.2. Plant material

The stems of *K. coccinea* were collected in the Menglun region of Yunnan Province, P. R. China, in September 2009 and identified by Prof. Xi-Wen Li at the Kunming Institute of Botany. A voucher specimen (KIB 20090901) was deposited in the Herbarium of the Kunming Institute of Botany, Chinese Academy of Sciences.

Table 4
Cytotoxicity of compounds **1–11** against Human Tumor Cell Lines (IC₅₀ values in μ M).

compound ^a	HL-60	SMMC-7721	A-549	MCF-7	SW-480	HeLa
2	13.43	>40	37.94	16.76	34.80	21.20
cis-platin ^b	1.93	11.83	12.40	18.34	18.10	8.93

^a Compounds **1** and **3–11** were inactive (IC₅₀ > 40 μ M) for all tumor cell lines.

^b Positive control substance.

4.3. Extraction and isolation

The air-dried and powdered stems (9 kg) of *K. coccinea* were extracted with 70% aqueous acetone by maceration (45 L × 3, each extraction lasted 3 days) at room temperature. Solvent removal was performed under reduced pressure to give a crude extract, which was then suspended in water and sequentially partitioned with EtOAc and *n*-BuOH, respectively. The EtOAc extract (450 g) was subjected to a silica gel column with a step-wise gradient elution of CHCl₃–acetone (1:0–0:1, v/v) to yield six fractions (A–F).

Fraction B (150 g) was further separated by an RP-C₁₈ silica gel column with mixtures of MeOH–H₂O (30–100%, v/v) to afford seven major fractions (B₁–B₇). Then, fraction B₆ (40 g) was applied to RP-C₁₈ silica gel CC with a gradient of MeOH–H₂O (65–100%, v/v) to obtain nine fractions (B₆₋₁–B₆₋₉). Fraction B₆₋₈ (25 g) was chromatographed over silica gel CC eluted with petroleum ether–acetone (5:1–2:1), giving eight minor subfractions (B₆₋₈₋₁–B₆₋₈₋₈). Subfraction B₆₋₈₋₃ (2 g) was also applied to successive semi-preparative HPLC using CH₃CN–H₂O (82:18, v/v, 3 mL/min) and MeOH–H₂O (88:12, v/v, 3 mL/min) respectively, yielding compounds **1** (13.5 mg) and **2** (24.6 mg). Subfraction B₆₋₈₋₄ (2.9 g) was further purified by repeated semi-preparative HPLC with CH₃CN–H₂O (85:15, v/v, 3 mL/min), and followed with MeOH–H₂O (80:20, v/v, 3 mL/min) to obtain compounds **3** (42.1 mg), **6** (11.4 mg), **7** (10.2 mg), and **11** (20.6 mg). Compounds **4** (12.7 mg), **5** (45.4 mg), and **12** (11.0 mg) were isolated from subfraction B₆₋₈₋₆ (1.6 g) by semi-preparative HPLC using MeOH–H₂O (90:10, v/v, 3 mL/min). Fraction B₇ (75 g) was partially subjected to semi-preparative HPLC using MeOH–H₂O (92:8, v/v, 3 mL/min) as eluent to yield seven subfractions (B₇₋₁–B₇₋₇). Subfraction B₇₋₄ (750 mg) was finally purified by semi-preparative HPLC with CH₃CN–H₂O (90:10, v/v, 3 mL/min) to give compounds **8** (7.8 mg), **9** (5.3 mg), **10** (4.3 mg), and **13** (3.1 mg).

4.3.1. Kadococcinone G (**1**)

White, amorphous powder; [α]_D²⁶ –96.7 (MeOH, *c* 0.15); UV (MeOH) λ_{\max} (log ϵ) = 204 (4.06) nm; IR ν_{\max} = 3439, 2956, 2934, 1734, 1633, 1460, 1378, 1248, 1201, 1181, 1054, 1028, 986, 608 cm⁻¹; For ¹H and ¹³C NMR data, see Tables 1 and 3; HRESIMS *m/z* 579.3658 [M + Na]⁺ (calcd for C₃₄H₅₂O₆Na, 579.3656).

4.3.2. Kadococcinone H (**2**)

White, amorphous powder; [α]_D²⁶ –45.3 (MeOH, *c* 0.10); UV (MeOH) λ_{\max} (log ϵ) = 204 (4.05) nm; IR ν_{\max} = 3442, 2955, 2934, 2881, 1736, 1636, 1460, 1379, 1246, 1183, 1052, 1025, 984, 606 cm⁻¹; For ¹H and ¹³C NMR data, see Tables 1 and 3; HRESIMS *m/z* 579.3663 [M + Na]⁺ (calcd for C₃₄H₅₂O₆Na, 579.3656).

4.3.3. Kadococcinone I (**3**)

White, amorphous powder; [α]_D²³ –128.3 (MeOH, *c* 0.10); UV (MeOH) λ_{\max} (log ϵ) = 205 (4.16) nm; IR ν_{\max} = 3447, 2953, 2929, 2878, 1726, 1635, 1550, 1461, 1428, 1381, 1247, 1029, 615 cm⁻¹; For ¹H and ¹³C NMR data, see Tables 1 and 3; HRESIMS *m/z* 513.3570 [M – H]⁻ (calcd for C₃₂H₄₉O₅, 513.3585).

4.3.4. Kadococcinone J (**4**)

White, amorphous powder; [α]_D²⁶ –132.8 (MeOH, *c* 0.05); UV (MeOH) λ_{\max} (log ϵ) = 204 (4.00) nm; IR ν_{\max} = 3445, 2957, 2921, 2851, 1732, 1712, 1637, 1549, 1461, 1378, 1250 cm⁻¹; For ¹H and ¹³C NMR data, see Tables 1 and 3; HRESIMS *m/z* 537.3550 [M + Na]⁺ (calcd for C₃₂H₅₀O₅Na, 537.3550).

4.3.5. Kadococcinone K (**5**)

White, amorphous powder; [α]_D²² –16.7 (MeOH, *c* 0.27); UV (MeOH) λ_{\max} (log ϵ) = 204 (3.99) nm; IR ν_{\max} = 3441, 2952, 2934,

2879, 1738, 1716, 1616, 1459, 1416, 1379, 1246, 1057, 1024, 989, 606 cm⁻¹; For ¹H and ¹³C NMR data, see Tables 1 and 3; HRESIMS *m/z* 537.3554 [M + Na]⁺ (calcd for C₃₂H₅₀O₅Na, 537.3550).

4.3.6. Kadococcinone L (**6**)

White, amorphous powder; [α]_D²⁶ +63.4 (MeOH, *c* 0.18); UV (MeOH) λ_{\max} (log ϵ) = 204 (4.06) nm; IR ν_{\max} = 3446, 2959, 2935, 2881, 1736, 1708, 1643, 1549, 1459, 1422, 1382, 1246, 1023, 608 cm⁻¹; For ¹H and ¹³C NMR data, see Tables 2 and 3; HRESIMS *m/z* 535.3394 [M + Na]⁺ (calcd for C₃₂H₄₈O₅Na, 535.3394).

4.3.7. Kadococcinone M (**7**)

White, amorphous powder; [α]_D²⁶ –55.3 (MeOH, *c* 0.04); UV (MeOH) λ_{\max} (log ϵ) = 204 (3.95) nm; IR ν_{\max} = 3444, 2970, 2930, 1733, 1736, 1633, 1458, 1426, 1384, 1248, 1087, 1047 cm⁻¹; For ¹H and ¹³C NMR data, see Tables 2 and 3; HRESIMS *m/z* 535.3395 [M + Na]⁺ (calcd for C₃₂H₄₈O₅Na, 535.3394).

4.3.8. Kadococcinone N (**8**)

White, amorphous powder; [α]_D²² +12.5 (MeOH, *c* 0.08); UV (MeOH) λ_{\max} (log ϵ) = 204 (3.93) nm; IR ν_{\max} = 3442, 2952, 2935, 2880, 1707, 1635, 1549, 1460, 1420, 1381, 1331, 1106, 592 cm⁻¹; For ¹H and ¹³C NMR data, see Tables 2 and 3; HRESIMS *m/z* 453.3362 [M – H]⁻ (calcd for C₃₀H₄₅O₃, 453.3374).

4.3.9. Kadococcinone O (**9**)

White, amorphous powder; [α]_D²² –60.8 (MeOH, *c* 0.10); UV (MeOH) λ_{\max} (log ϵ) = 205 (3.96) nm; IR ν_{\max} = 3452, 2951, 2927, 2880, 1640, 1460, 1384, 1064, 664 cm⁻¹; For ¹H and ¹³C NMR data, see Tables 2 and 3; HRESIMS *m/z* 455.3518 [M – H]⁻ (calcd for C₃₀H₄₇O₃, 455.3531).

4.3.10. Kadococcinone P (**10**)

White, amorphous powder; [α]_D²¹ –82.6 (MeOH, *c* 0.07); UV (MeOH) λ_{\max} (log ϵ) = 205 (3.95) nm; IR ν_{\max} = 3448, 2950, 2927, 2877, 1734, 1642, 1458, 1384, 1245, 1052, 1030, 608 cm⁻¹; For ¹H and ¹³C NMR data, see Tables 2 and 3; HRESIMS *m/z* 497.3622 [M – H]⁻ (calcd for C₃₂H₄₉O₄, 497.3636).

4.3.11. Kadococcinone Q (**11**)

White, amorphous powder; [α]_D²⁶ –95.4 (MeOH, *c* 0.04); UV (MeOH) λ_{\max} (log ϵ) = 204 (3.97) nm; IR ν_{\max} = 3441, 2952, 2931, 2877, 1732, 1631, 1461, 1426, 1383, 1248, 1107, 1030, 586 cm⁻¹; For ¹H and ¹³C NMR data, see Tables 2 and 3; HRESIMS *m/z* 537.3551 [M + Na]⁺ (calcd for C₃₂H₅₀O₅Na, 537.3550).

4.4. X-ray crystal structure analysis

A suitable crystal of **1** was obtained in CHCl₃ (with six drops of MeOH). Intensity data were acquired at 100 k on a Bruker APEX DUO diffractometer equipped with an APEX II CCD, using Cu *K* α radiation. Cell refinement and data reduction were performed by Bruker SAINT. The structure was solved by direct methods with SHELXS-97.¹⁸ Refinements were performed with SHELXL-97 using full-matrix least-squares, with anisotropic displacement parameters used for all the non-hydrogen atoms. The hydrogen atoms were located in the calculated positions and refined with a riding model. Molecular graphic was computed with PLATON. The crystallographic data for **1** (deposition No. CCDC 1470163) have been deposited in the Cambridge Crystallographic Data Centre. Copies of the data can be obtained free of charge on application to CCDC, 12 Union Road, Cambridge CB 1EZ, UK [fax: Int. + 44 (0) (1223) 336 033; e-mail: deposi@ccdc.cam.ac.uk].

Crystallographic data for 1: C₃₄H₅₂O₆, *M* = 556.76, orthorhombic, *a* = 9.8251(2) Å, *b* = 13.4462(2) Å, *c* = 48.0954(8) Å,

$\alpha = 90.00^\circ$, $\beta = 90.00^\circ$, $\gamma = 90.00^\circ$, $V = 6353.90(19) \text{ \AA}^3$, $T = 100(2) \text{ K}$, space group $P212121$, $Z = 8$, $\mu(\text{Cu K}\alpha) = 0.619 \text{ mm}^{-1}$, 38440 reflections measured, 11279 independent reflections ($R_{\text{int}} = 0.0317$). The final R_1 values were 0.0336 ($I > 2\sigma(I)$). The final $wR(F^2)$ values were 0.0882 ($I > 2\sigma(I)$). The final R_1 values were 0.0341 (all data). The final $wR(F^2)$ values were 0.0886 (all data). The goodness of fit on F^2 was 1.043. Flack parameter = 0.01(10). The Hooft parameter is 0.00(4) for 4840 Bijvoet pairs.

4.5. Cytotoxic assays

HL-60 (acute leukemia), SMMC-7721 (hepatic cancer), A-549 (lung cancer), MCF-7 (breast cancer), SW-480 (colon cancer), and HeLa (cervical cancer) human tumor cell lines were used in the cytotoxicity assays. All cells were cultured in RPMI-1640 or DMEM medium (Hyclone, Logan, UT, USA) supplemented with 10% fetal bovine serum (Hyclone) at 37°C in a humidified atmosphere containing 5% CO_2 . Cell viability was assessed by conducting colorimetric measurements of the amount of insoluble formazan formed in living cells based on the reduction of 3-(4,5-dimethylthiazol-2-yl)-5-(3-carboxymethoxyphenyl)-2-(4-sulfophenyl)-2H-tetrazolium (MTS) (Sigma, St. Louis, MO, USA).¹⁷ Briefly, 100 μL of adherent cells were seeded into each well of a 96-well cell culture plate and allowed to adhere for 12 h before drug addition, while suspended cells were seeded just before addition of the test compound, both with an initial density of 1×10^5 cells/mL in 100 μL medium. Each tumor cell line was exposed to the tested compound at various concentrations in triplicate for 48 h, with *cis*-platin as the positive control substance. After the incubation, MTS (100 μg) was added to each well, and the incubation continued for 4 h at 37°C . The cells were lysed with 100 μL of 20% SDS–50% DMF after removal of 100 μL of medium. The optical density of the lysate was measured at 490 nm in a 96-well

microtiter plate reader (Bio-Rad 680). The IC_{50} value of each compound was calculated by Reed and Muench's method.¹⁹

Acknowledgments

This work was supported by the National Natural Science Foundation of China (Nos. 81373290 and 21322204).

Appendix A. Supplementary data

Copies of ^1H and ^{13}C NMR spectra for all products. Supplementary data associated with this article can be found in the online version, at <http://dx.doi.org/10.1016/j.tet.2017.03.087>. These data include MOL files and InChIKeys of the most important compounds described in this article.

References

1. Xiao WL, Li RT, Huang SX, Pu JX, Sun HD. *Nat Prod Rep*. 2008;25:871–891.
2. Shi YM, Xiao WL, Pu JX, Sun HD. *Nat Prod Rep*. 2015;32:367–410.
3. Gao XM, Pu JX, Huang SX, et al. *J Nat Prod*. 2008;7:1182–1188.
4. Yang JH, Wen J, Du X, et al. *Tetrahedron*. 2010;66:8880–8887.
5. Pu JX, Xiao WL, Lu Y, et al. *Org Lett*. 2005;7:5079–5082.
6. Liang CQ, Shi YM, Luo RH, et al. *Org Lett*. 2012;14:6362–6365.
7. Liang CQ, Shi YM, Li XY, et al. *J Nat Prod*. 2013;76:2350–2354.
8. Liang CQ, Shi YM, Wang WG, et al. *J Nat Prod*. 2015;78:2067–2073.
9. Yang JH, Pu JX, Wen J, et al. *Phytochemistry*. 2015;109:36–42.
10. Hu ZX, Shi YM, Wang WG, et al. *Org Lett*. 2015;17:4616–4619.
11. Hu ZX, Hu K, Shi YM, et al. *J Nat Prod*. 2016;79:2590–2598.
12. Hu ZX, Shi YM, Wang WG, et al. *Org Lett*. 2016;18:2284–2287.
13. Asakawa J, Kasai R, Yamasaki K, Tanaka O. *Tetrahedron*. 1977;3:1935–1939.
14. Stuppner H, Müller EP. *Phytochemistry*. 1993;3:1139–1145.
15. Dong K, Pu JX, Du X, et al. *Tetrahedron*. 2012;68:4820–4829.
16. Yang XW, Li SM, Wu L, et al. *Org Biomol Chem*. 2010;8:2609–2616.
17. Monks A, Scudiero D, Skehan P, et al. *J Natl Cancer Inst*. 1991;83:757–766.
18. Sheldrick GM, Schneider TR. *Method Enzymol*. 1997;277:319–343.
19. Reed LJ, Muench H. *Am J Hyg*. 1938;27:493–497.